

TRANSVERSE IMPEDANCES OF CAVITIES AND COLLIMATORS*

S. A. KHEIFETS, K. L. F. BANE, H. BIZEK

Stanford Linear Accelerator Center, Stanford University, Stanford, CA 94305

Introduction

When an ultra-relativistic charge moves past a discontinuity in an accelerator vacuum chamber, electromagnetic fields are excited. A test charge following behind the exciting charge will, in general, experience a longitudinal kick (affecting its energy) and a transverse kick from these fields. The interaction can be characterized by the wakefield or the impedance of the structure. Either of these functions are useful for studying the current dependent behavior of a bunch of particles in an accelerator.

It has long been possible to compute the longitudinal and transverse impedances of the periodic disk-loaded structure,^{1,2} as well as the impedances of cylindrically symmetric cavities with arbitrary shape, up to the tube cut-off frequency.^{3,4} More recently, the computation of the longitudinal impedance of simple cavities⁵⁻⁷ and collimators,^{6,7} and of arbitrarily shaped cylindrically symmetric structures⁸ has been demonstrated, including frequencies above cut-off.

In Ref. 9 the method of field matching is used to calculate the transverse impedance of a simple, cylindrically symmetric, perfectly conducting cavity with long beam tubes. The structure is divided into two subregions separated by a longitudinal cut. The fields are given as an expansion with unknown coefficients in the two subregions. The coefficients are then found by matching the fields along the cut. In the present paper, field matching will also be used to compute the transverse impedance of simple structures. The subregions, however, will be separated by radial cuts, allowing us to consider the case of a simple collimator as well as that of the simple cavity. Furthermore, our cut allows the two beam tubes to have differing radii (See Fig. 1).

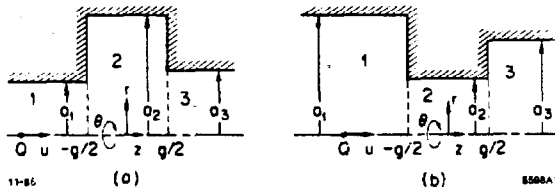


Fig. 1. Cylindrically symmetric structures considered in the present work: a) a cavity and b) a collimator.

We will briefly describe our method and present some early results. More details will be forthcoming in a future paper.

The Current Sources

Consider an ultra-relativistic particle of charge Q moving at speed βc parallel to the z axis of a cylindrically symmetric

structure. Let the transverse position of the particle be at $r = h$ and $\theta = 0$. The current density is then given as

$$j_z = \sum_{m=0}^{\infty} j_{zm} = \frac{Q\beta c}{\pi r} \delta(r-h) \delta(z-\beta ct) \sum_{m=0}^{\infty} \frac{\cos m\theta}{1 + \delta_{m0}} \quad (1)$$

with δ_{m0} the Kronecker delta. The $m = 0$ term in the sum drives monopole modes, the $m = 1$ term drives dipole modes, etc. If the beam moves close to the structure axis the monopole modes dominate the longitudinal effect, whereas the dipole modes dominate the transverse effect. We limit our study here to the dipole modes, though the method that we use can easily be modified to calculate higher multipole modes.

For calculating the transverse impedance we take as driving term the Fourier transform of the dipole component of j_z

$$\tilde{j}_{z1} = \int_{-\infty}^{\infty} j_{z1} \exp(ikct) dt = \frac{Q}{\pi r} \delta(r-h) \cos \theta \exp(ikz/\beta) \quad (2)$$

with the wave number $k = \omega/c$. Once the resulting fields are known, the transverse impedance is given by

$$iZ_r = \frac{1}{Qh \cos \theta} \int_{-\infty}^{\infty} [\tilde{E}_r - \beta c \tilde{H}_\theta] \exp(-ikz/\beta) dz \quad (3)$$

Field Expansions

The structures of interest to us are composed of simple cylindrical subregions that include the axis. In any such subregion ℓ with pipe radius a_ℓ , the Hertz potentials of the radiation fields excited by the point charge can, in general, be expanded into a series of cylindrical waves with unknown coefficients as¹⁰

$$\begin{aligned} \tilde{\Pi}_{z\ell} &= -\cos \theta \sum_n J_1\left(\frac{\nu_n r}{a_\ell}\right) [C_{\ell n}^- \exp(-i\lambda_{\ell n} z) + C_{\ell n}^+ \exp(i\lambda_{\ell n} z)] \\ \tilde{\Pi}_{z\ell}^* &= -\sin \theta \sum_n J_1\left(\frac{\mu_n r}{a_\ell}\right) [D_{\ell n}^- \exp(-i\sigma_{\ell n} z) + D_{\ell n}^+ \exp(i\sigma_{\ell n} z)] \end{aligned} \quad (4)$$

The propagation constants are given by

$$\lambda_{\ell n} = \sqrt{k^2 - \frac{\nu_n^2}{a_\ell^2}} \quad \text{and} \quad \sigma_{\ell n} = \sqrt{k^2 - \frac{\mu_n^2}{a_\ell^2}} \quad (5)$$

with ν_n and μ_n representing the n^{th} root of J_1 and J_1' respectively.

The coefficients for radiated waves moving in the positive z direction are C_n^+ , D_n^+ , whereas those for waves moving in

* Work supported by the US Department of Energy, contract DE - AC03 - 76SF00515.

the negative z direction are C_n^-, D_n^- . Thus, in subregion 1 of the cavity or collimator (see Fig. 1) all the former coefficients must be zero, while in subregion 3 all the latter coefficients are zero. Only in the middle subregion do we need all four sets of coefficients. Note that the propagation constants need to be defined with negative imaginary parts, to satisfy the Sommerfeld radiation condition.

The Fourier transforms of the vector and scalar potentials are given by

$$\begin{aligned}\tilde{\mathbf{A}}_\ell &= -ik\tilde{\Pi}_\ell + \nabla \times \tilde{\Pi}_\ell + \hat{z} \frac{2Q}{\pi c} F_\ell(r) \exp(ikz/\beta) \cos \theta \\ \tilde{\Phi}_\ell &= -\nabla \cdot \tilde{\Pi}_\ell + \frac{2Q\beta}{\pi c} F_\ell(r) \exp(ikz/\beta) \cos \theta\end{aligned}\quad (6)$$

with

$$F_\ell(r) = \begin{cases} I_1(\tau r)[K_1(\tau h) - I_1(\tau h)K_1(\tau a_\ell)/I_1(\tau a_\ell)] & r \leq h \\ I_1(\tau h)[K_1(\tau r) - I_1(\tau r)K_1(\tau a_\ell)/I_1(\tau a_\ell)] & r > h, \end{cases}\quad (7)$$

$$\tau = k/\beta\gamma \quad (8)$$

The last terms in Eq. (6) are the source terms. The functions I_1, K_1 are the modified Bessel functions of the 1st order.

From the scalar and vector potentials we get the electric and magnetic fields of region ℓ in the usual manner. Note that the boundary conditions for a perfect conductor are automatically satisfied at $r = a_\ell$.

Field Matching

The cavities and collimators that we will consider can be decomposed into three simple cylindrical subregions (see Fig. 1). In order to solve for the unknown coefficients in our field expansions we first match the four tangential field components $\tilde{E}_r, \tilde{E}_\theta, \tilde{H}_r, \tilde{H}_\theta$, at the boundaries between adjoining regions. In addition, \tilde{E}_r and \tilde{E}_θ are set to zero on a radial wall. We then eliminate r from these equations by performing a definite integration over r .

For example, for the cavity of Fig. 1a, at $z = -g/2$ we set

$$\begin{aligned}\tilde{E}_{r2}, \tilde{E}_{\theta2} &= \begin{cases} \tilde{E}_{r1}, \tilde{E}_{\theta1} & r < a_1 \\ 0 & a_1 \leq r \leq a_2 \end{cases} \\ \tilde{H}_{r2}, \tilde{H}_{\theta2} &= \tilde{H}_{r1}, \tilde{H}_{\theta1} \quad r < a_1\end{aligned}\quad (9)$$

Both sides of these equations are multiplied by $J_1(\nu_i r/a_p)r^2 dr$ and then integrated from $r = 0$ to $r = a_p$, with $p = 2$ for the first two equations, $p = 1$ for the final two equations. The corresponding procedure is then applied at the boundary at $z = g/2$.

We are finally left with eight infinite sets of equations involving the eight sets of unknown coefficients $C_{1n}^-, D_{1n}^-, C_{2n}^-, D_{2n}^-, C_{2n}^+, D_{2n}^+, C_{3n}^+, D_{3n}^+$. The problem can be written in matrix notation as

$$\mathbf{M}\mathbf{x} = \mathbf{b} \quad (10)$$

with \mathbf{M} an infinite matrix, \mathbf{x} and \mathbf{b} vectors of infinite dimension, with \mathbf{x} representing the unknown coefficients. After truncating the matrix and vectors to finite size, Eq. (10) is solved numerically for \mathbf{x} .

Results

Two computer codes have been written to calculate the transverse impedances of a simple cavity and a scraper at discrete values of k according to the method described above. Due to the memory limitation of our computer the sums in Eq. (4) are truncated at 50 terms. For the examples to be presented here, however, the impedance results remain essentially unchanged when only 20 terms are included in the computation. For simplicity, we restrict ourselves to the case of $\beta = 1$ in our examples.

For our first example we give the impedance of a cavity with $a_1 = a_3$, $a_2/a_1 = 6.58$, $g/a_1 = 3.97$. The imaginary part of Z_r below the TE₁₁ cut-off frequency, $ka_1 = 1.84$, is given in Fig. 2. Its value at the origin is -81Ω . The frequencies where $\Im m(Z_r)$ changes abruptly from a large negative to a large positive value are the resonances. We have broken the curve at these points. The resonances are at $ka_1 = 0.58, 0.83, 0.97, 1.06, 1.12, 1.30, 1.58, 1.65$ and 1.69 . These values agree with the results given by the computer code TRANSVRS.² In this range, the real part of Z_r is given by a sequence of delta functions, and thus cannot be found directly by our method.

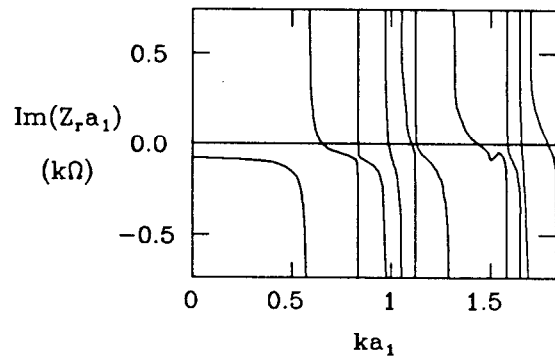


Fig. 2. $\Im m(Z_r)$ below cut-off for a cavity with $a_1 = a_3$, $a_2/a_1 = 6.58$, $g/a_1 = 3.97$.

$\Re e(Z_r)$ above cut-off for this structure is given in Fig. 3. As in the longitudinal case^{5,7} we find a few sharp (but finite) peaks just above cut-off, in the present case at $ka_1 = 1.85$ and 2.04 , with broader peaks occurring at higher frequencies.

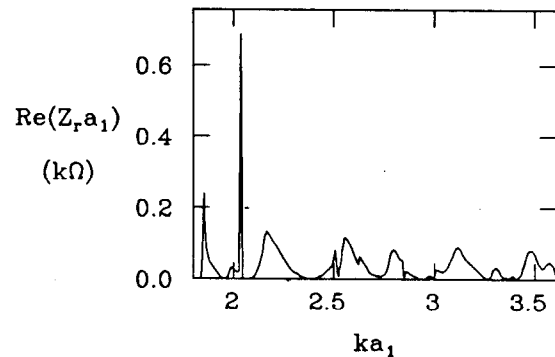


Fig. 3. $\Re e(Z_r)$ above cut-off for a cavity with $a_1 = a_3$, $a_2/a_1 = 6.58$, $g/a_1 = 3.97$.

As a second example we give the dipole impedance of a single convolution of a rectangular bellows (See Fig. 4). The dimensions are $a_1 = a_3$, $a_2/a_1 = 1.212$, $g/a_1 = 0.0667$. As in the longitudinal case⁵ the impedance is dominated by one

large, somewhat broad resonance, centered above the lowest TM tube cut-off. The peak is centered at $ka_1 = 6.11$; its maximum value is 11.75Ω . Its position roughly agrees with $k(a_2 - a_1) = \pi/2$, which yields $ka_1 = 7.4$. The Q , defined as the central frequency divided by twice the full width at half maximum, is 5. Smaller peaks are found at $ka_1 = 3.88$ and $ka_1 = 7.26$, just above the first two TM1 tube cut-off frequencies, 3.83 and 7.02. The value of $a_1 \Im m(Z_r(0))$ is -0.74Ω .

For comparison, we have also used the computer code TBCI¹¹ to calculate the wakefield of a short Gaussian bunch, with bunch length $\sigma_z = 0.06a_1$, up to a distance of $12a_1$. Taking the Fast Fourier Transform of this function, then multiplying by $\exp(k^2\sigma_z^2/2)$ yields Z_r . (We will denote this as the FFT method. For a discussion of this method, see for example Ref. 12.) The results of this calculation are given as crosses in Fig. 4. Although it is difficult to get high resolution by the FFT method, we see that the results of the two methods compare quite well. Possibly the only important difference is in the value of $a_1 \Im m(Z_r(0))$. Here the FFT method yields -1.28Ω .

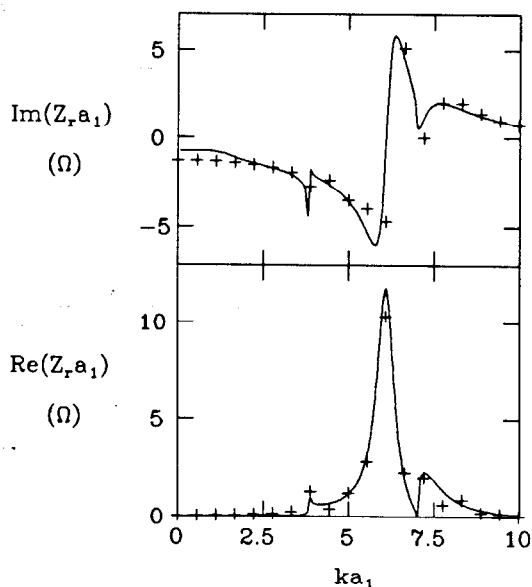


Fig. 4. $\Im m(Z_r)$ (top) and $\Re e(Z_r)$ (bottom) for a single convolution of a bellows with $a_1 = a_3$, $a_2/a_1 = 1.212$, $g/a_1 = 0.0667$. The crosses give the results of the FFT method for comparison.

As a final example we give the dipole impedance of a single iris in a tube. The dimensions are $a_1 = a_3$, $a_2/a_1 = 0.281$ and $g/a_1 = 0.122$. The impedance for this obstruction is shown in Fig. 5. Two narrow peaks can be seen near the first two TM1 cut-offs of the tube. One large resonance, at $ka_1 = 3.81$, has a peak value of $a_1 \Re e(Z_r) = 14.61 \text{ k}\Omega$ and $Q = 200$. A smaller resonance, at $ka_1 = 7.015$, has a peak value of $a_1 \Re e(Z_r) = 0.76 \text{ k}\Omega$ and $Q = 700$. Thus we see that a single iris can trap modes with very high Q values. In between these two narrow resonances we find a broad shoulder. The value of $a_1 \Im m(Z_r(0))$ is $-0.22 \text{ k}\Omega$.

We have again calculated the impedance by the FFT method, for comparison. The wakefield used was that of a bunch with length $\sigma_z = 0.1a_1$, computed out to $20a_1$. We have roughly twice the resolution of the previous example. On the whole, the results of the two methods agree. The FFT method yields a

value of $a_1 \Im m(Z_r(0)) = -0.19 \text{ k}\Omega$, comparing well with the field matching results. The FFT method, however, cannot resolve the very narrow resonance at $ka_1 = 7.01$. The major discrepancies in the results are that, unlike the field matching method, the FFT method predicts a rather broad tail below the first resonance and a small, broad peak at $ka_1 = 5.73$.

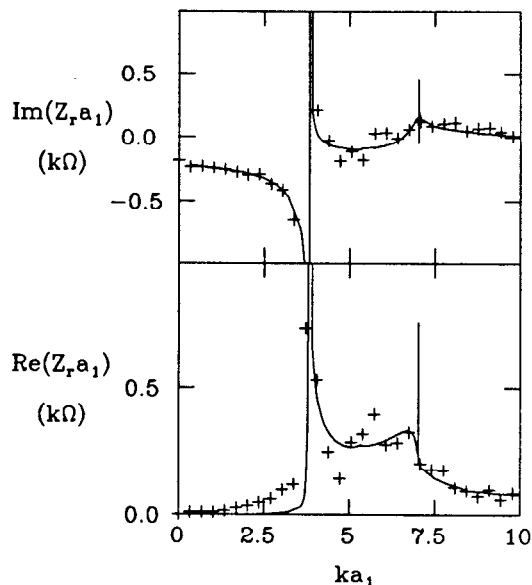


Fig. 5. $\Im m(Z_r)$ (top) and $\Re e(Z_r)$ (bottom) for an iris in a tube with $a_1 = a_3$, $a_2/a_1 = 0.281$, $g/a_1 = 0.122$. The peak value of $a_1 \Re e(Z_r)$ is $14.61 \text{ k}\Omega$, centered at $ka_1 = 3.83$. The crosses give the FFT results.

Acknowledgements

The authors thank B. Woo for help with the programming.

References

1. E. Keil, *Nucl. Instr. Meth.* **100**, 419 (1972).
2. K. Bane, B. Zotter, Proceedings of the 11th Int. Conf. on High Energy Accelerators, CERN (Birkhäuser Verlag, Basel, 1980), p. 581.
3. K. Halbach, R.F. Holsinger, *Particle Accelerators* **7**, 213 (1976).
4. T. Weiland, *Nucl. Instr. Meth.* **216**, 329 (1983).
5. H. Henke, CERN-LEP-RF/85-41 (1985).
6. L. Vos, CERN-SPS/86-21 (1986).
7. S. Kheifets, SLAC-PUB-4133 (1986).
8. U. van Rienen, T. Weiland, Proceedings of the 1986 Linear Accelerator Conf., SLAC-Report-303, 289 (1986).
9. H. Henke, *IEEE Trans. Nucl. Sci.* **NS-32**, 2335 (1985).
10. J.A. Stratton, "Electromagnetic Theory", (McGraw-Hill, N.Y., 1941), p. 524.
11. T. Weiland, DESY 82-015 (1982) and *Nucl. Instr. Meth.* **212**, 13 (1983).
12. K. Bane, R. Ruth, SLAC-PUB-3862; SLAC/AP 45 (1985).